Hindawi
Advances in Civil Engineering
Volume 2018, Article ID 2632549, 10 pages
https://doi.org/10.1155/2018/2632549

Research Article

Research of Rock Burst Risk Induced by Mining and Field Case in Anticlinal Control Area

Shitan Gu,[1,2] Zhimin Xiao,[3,4] Bangyou Jiang,[1,2] Ruifeng Huang,[5] and Peng Shan[3,4]

[1]*State Key Laboratory of Mining Disaster Prevention and Control Co-founded by Shandong Province and the Ministry of Science and Technology, Shandong University of Science and Technology, Qingdao, Shandong 266590, China*
[2]*College of Mining and Safety Engineering, Shandong University of Science and Technology, Qingdao, Shandong 266590, China*
[3]*College of Civil and Transportation Engineering, Hohai University, Nanjing 210098, China*
[4]*Institute of Engineering Safety and Disaster Prevention, Hohai University, Nanjing 210098, China*
[5]*Inner Mongolia Urban Planning and Municipal Engineering Design Research Institute, Hohhot 010070, China*

Correspondence should be addressed to Zhimin Xiao; sdustxiaozhimin@163.com and Bangyou Jiang; jiangbangyou123@163.com

Received 26 February 2018; Revised 30 August 2018; Accepted 27 September 2018; Published 22 October 2018

Academic Editor: Ottavia Corbi

Stress concentration caused by tectonic stress and mining disturbance in coal mines induces a unique type of rock burst. No. 3201 working face controlled by an anticline structure in the Shandong mining area is used as the research background. The formation mechanism for anticlines is analyzed. Theoretical research shows that the bigger the tectonic couple is, the smaller the foundation stiffness, and the greater the bending degree and elastic strain energy of the coal will be. The distribution characteristics of abutment pressure and maximum principle stress in anticlinal control areas are analyzed using UDEC numerical software. The results show that rock bursts result from interactions between abutment pressure and residual tectonic stress. The "connection-overlay-separation" phenomenon of abutment pressure presents with working face advancement. Furthermore, the energy criterion for rock burst initiation is established based on the energy principle. Residual energy "E_0 E_C" and rock burst danger characteristics during mining are discussed. Based on the simulation results, microseismic monitoring data for No. 3201 working face are analyzed, and the law of microseismic energy is consistent with the variation law for the residual energy "E_0 E_C" at the peak of the simulated abutment pressure. The microseismic energy and frequency are higher during mining, increasing the risk of rock burst events. It can provide scientific basis for prevention and control of rock burst.

1. Introduction

Rock bursts are common dynamic disasters in coal mining. The elastic energy of coal and rock is released in the form of a sudden, sharp, and violent burst, with instantaneous destruction and rock expulsion. The intensity of a rock burst and the resulting damage are more prominent in abnormal stress areas of anticline structures. Since the first report of a British rock burst in 1738, the disaster has spread all over the world and presents a serious threat to safe mining [1–4]. Coal and rock geological history in anticline structures highlights the transformation and presents the geological structure characteristics of rock burst events. Complex tectonic stress fields and mining stress fields overlap in these structures, which increases the complexity of rock bursts and the difficulty of controlling them. Therefore, research on the mechanism of rock burst prevention has become one of the key scientific and technical problems in the field of rock mechanics [5, 6].

Many scholars at home and abroad have carried out thorough research on the mechanism and prevention of rock bursts, with remarkable results. A series of theories, such as energy theory, stiffness theory, strength theory, and impact tendency theory, have been proposed [7–10]. At present, research on the theory of rock burst events is mainly focused on the crack propagation law, energy damage, and the stability of the local area on the basis of fracture mechanics, damage theory, and catastrophe theory. Dyskin et al. [11, 12]

reported that roadways surrounding rock are affected by the concentrated compressive stress, which leads to the further growth and coalescence of cracks, finally causing the cracked surface to separate, and inducing rock burst by the buckling failure induces the impact. Based on the Griffith energy theory and the associated criterion, crack propagation is coupled with material damage, and the critical stress R value of a rock burst can be determined [13]. Some scholars [14–17] established a catastrophe structure instability model for coal and rock masses and analyzed the stress and stiffness of the surrounding rock as well as the expansion energy of coal and rock masses.

The fold rock burst is a special type of rock burst that occurs in coal and rock masses. Because of the special environment of coal and rock masses and the stress environment, the cause of rock bursts in this area is complex. Wrinkles are usually the result of slow deformation of rock strata under the influence of horizontal pressure in the region; that is, a fold is formed under longitudinal bending [18]. Near the fold structure, the tectonic stress field is dominated by horizontal stress, and the mining stress fields are superimposed on each other. This produces more intense stress differentiation, resulting in high energy accumulation and leading to crack propagation, coalescence, and an irreversible process of nonlinear dynamics. Mining in the fold area can easily cause the release of stress-induced rock bursts, which often occurs in the axis of the fold [19–21]. According to the statistics released by the Tianchi Coal Mine and Mentougou Mine, rock bursts occurred 78 times in the geological structure area and 31 times in the anticlinal belt, accounting for 40% of rock burst events. The research indicates that the axis of the anticline, which has a wing angle greater than 45 degrees, and the turning position form tectonic stress concentration and accumulate a great deal of elastic energy. The rock burst induced by mining occurs in these areas [22–24]. To address the problems such as the lack of early warning methods and prevention technology for rock bursts, many scholars have conducted thorough research. As a result, rock bursts can be effectively controlled to a certain extent [25–29].

At present, the mechanism of fault rock bursts has received the most attention. However, there are few studies on evolution laws for tectonic stress, mining stress, and energy evolution and the control mechanism for tectonic rock bursts. No. 3201 working face controlled by an anticline structure is used as the research background in this paper. The mechanical model for the anticline is constructed, and a theoretical solution for deflection and the elastic strain energy of the rock beam are deduced. The internal factors that affect the formation of the anticline and its impact are then discussed. A numerical model of the anticline is also established using UDEC software, and abutment pressure and the maximum principal stress distribution characteristics of the anticline under working faces with different mining distances are simulated and analyzed. Then, based on the energy principle, the criterion for rock burst initiation is established, and rock burst danger before the working face in the anticline-controlled area is studied. In addition, a microseismic monitoring system is used to monitor the microseismic events during the mining process of No. 3201 working face, as well as when the working face is close to and far from the axis of the anticline. The characteristics of microseismic events and the rock burst risk are discussed.

2. Formation Mechanism of Anticline Structure

2.1. Theoretical Solution for Anticline Formation. In a deep stratum environment, tectonic stress is the maximum principal stress, and the direction is generally at a certain angle to the horizontal with the tendency of the coal seam. Fold formation is closely related to tectonic stress. References [30–32] studied the causes of the Yanshan structure in the Hubei province in China, the Wuxu mine field in the Guangxi province in China, and the Taiyuan tilting structure in the Shanxi province in China. The results show that tectonic coupling is the source of fold formation. Therefore, the coal seam is equivalent to the Winker elastic support and the uniform load of infinite beams, and tectonic coupling is simplified to a single couple. The fold mechanical model is shown in Figure 1. The left side of the w-axis can forms a syncline structure, and the right side can form an anticline structure. The arbitrary microsection dx in the anticlinal model is intercepted, and the width of the microsection is 1 so that we can analyze the model stress, as shown in Figure 2.

Based on the force balance of the microsection dx,

$$\begin{cases} \sum F_w = 0 \Rightarrow F_s + dF_s - F_s + kw\,dx - \gamma h\,dx = 0, \\ \sum M = 0 \Rightarrow M - M - dM + \left(F_s + dF_s\right) dx \\ \quad + kw\dfrac{dx^2}{2} - \gamma h\dfrac{dx^2}{2} = 0, \end{cases} \tag{1}$$

where F_s is the shear force; γ is the rock density; h is the depth of the rock stratum; M is the rock moment of the couple; k is the foundation stiffness; and w is the deflection.

Simplification of Formula (1):

$$\begin{cases} \dfrac{dF_s}{dx} = \gamma h - kw, \\ \dfrac{dM}{dx} = F_s. \end{cases} \tag{2}$$

From the mechanics of materials, we obtain

$$EI\frac{d^2w}{dx^2} = M, \tag{3}$$

where E is the modulus of elasticity and I is the moment of inertia.

By means of Formulas (2) and (3), a deflection equation for dx supported by the Winker elastic foundation is obtained:

$$EI\frac{d^4w}{dx^4} + kw = \gamma h. \tag{4}$$

From natural boundary conditions and continuous conditions for the beam, the solution for Formula (4) and dx strain energy can be expressed as

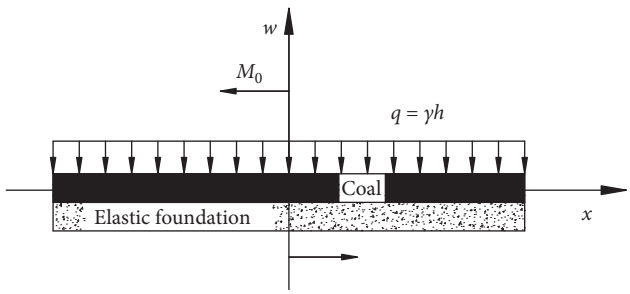

Figure 1: Mechanical model of a fold.

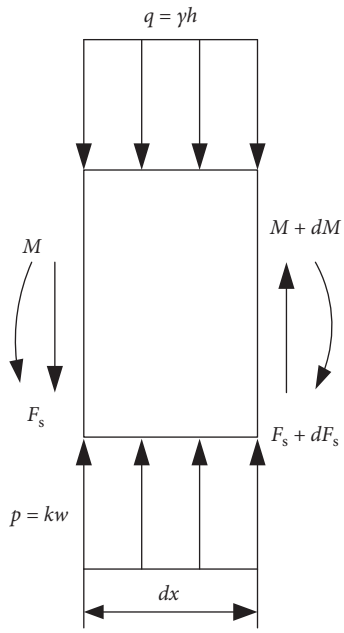

Figure 2: Stress analysis diagram of the anticlinal microsection dx.

$$w = \frac{M_0\sqrt{k/4EI}}{k} e^{-\sqrt[4]{\frac{k}{4EI}}x} \sin \sqrt[4]{\frac{k}{4EI}}x + \frac{\gamma h}{k}, \tag{5}$$

$$dV_\varepsilon = \frac{M^2(x)\,dx}{2EI}, \tag{6}$$

where dV_ε is the strain energy of the rock beam macrosection dx.

By means of Formulas (3), (5), and (6), anticlinal strain energy can be defined as follows:

$$\begin{aligned} V &= \int_0^x dV_\varepsilon = \int_0^x \left(\frac{M_0^2 e^{-2\alpha t}\cos^2 \alpha t}{8EI}\right) dt \\ &= \frac{M_0^2}{64EI\alpha}\left(3 - e^{-2\alpha x} - e^{-2\alpha x}\cos 2\alpha x\right), \end{aligned} \tag{7}$$

where α is the characteristic coefficient, $\alpha = \sqrt[4]{k/4EI}$ and t only represents integral variable in the article.

In summary, the deflection of rock and the strain energy of microsection dx are closely related to the bending moment and location. If the tectonic force is greater and the bending stiffness is smaller, the rock beam deflection and strain energy will increase. When mining disturbance occurs at the location, a great deal of energy stored in the coal and rock will be released instantaneously, which will easily induce rock burst.

2.2. Variation of Anticlinal Elastic Strain Energy under Different Factors. According to the geological data for No. 3 coal seam and No. 3201 working face in Shandong Mine, China, the mining area is affected by anticline structures. The relevant parameters for the calculation are as follows. The average depth of coal is $h = 800$ m. The mean thickness of the coal seam is 6 m. The elastic modulus $E = 2.8$ GPa of coal is measured using the TAW-2000 electrohydraulic servo testing machine, and flexural rigidity is $EI = 5.04 \times 10^{10}$ N·m^2. The volumetric weight is $\gamma = 25$ kN/m^3. For the foundation stiffness, $k = 10$ GPa, 15 GPa, and 20 GPa are used. Based on the measured results for in situ stress using the stress-relieving method, the ratio of the maximum horizontal stress to the vertical stress is 1.3–3.2. The tectonic stress concentration factor is taken as 1, 2, and 4, while the corresponding structural couple is $M_0 = 2.0 \times 10^9$ N·m, 4.0×10^9 N·m, and 8×10^9 N·m. In order to facilitate the analysis using the control variable method, anticline formation and energy accumulation are researched with variations in tectonic stress and foundation stiffness.

2.2.1. Different Tectonic Couple.

(1) Analysis of anticlinal deflection. When the foundation stiffness is $k = 10$ GPa, the tectonic couple is taken as $M_0 = 2.0 \times 10^9$ N·m, 4.0×10^9 N·m, and 8.0×10^9 N·m. The corresponding anticlinal deflection curve is shown as Figure 3.

It can be seen from Figure 3 that the uplift degree of the anticline is increased with the increase of tectonic coupling when foundation stiffness is constant. The deflection peak is located 2 m from the center of the w-axis. As the distance from the center of the w-axis increases, the deflection value of anticlinal with different couple decreases and gradually becomes consistent. However, a certain deflection value remains. The greater the anticline uplift is, the greater the dip angle of the working face will be.

(2) Analysis of anticlinal elastic strain energy. When the foundation stiffness is $k = 10$ GPa, the tectonic couple is taken as $M_0 = 2.0 \times 10^9$ N·m, 4.0×10^9 N·m, and 8.0×10^9 N·m. The corresponding anticlinal elastic strain energy curve is shown in Figure 4.

It can be seem from Figure 4 that the anticlinal elastic strain energy increases with the increase of the tectonic coupling when the foundation stiffness is constant. With the increase of distance from the center of the w-axis, elastic strain energy presents a "logarithmic curve" change trend; that is, it appears to increase first and then gradually becomes gentle. Since there is still a certain amount of uplift deformation away from the center of the w-axis, a large amount of elastic energy is stored. When mining activity occurs at the anticline control area, the superimposition of the deformation energy caused by mining stress and the

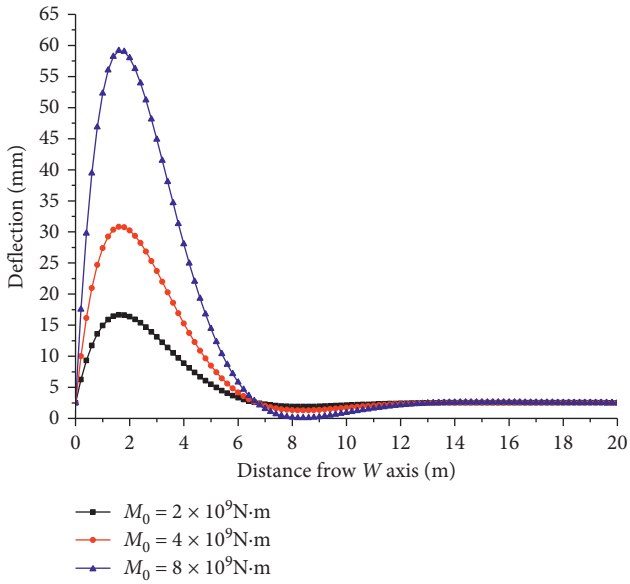

Figure 3: Distribution curves of anticlinal deflection with different tectonic couple.

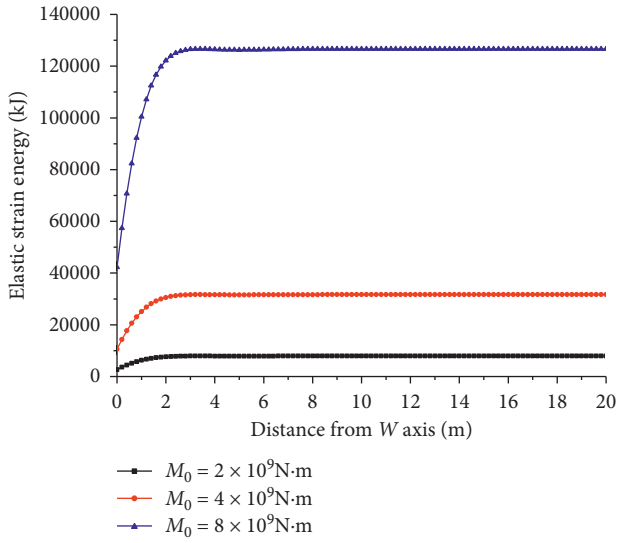

Figure 4: Distribution curves of anticlinal elastic strain energy with different tectonic couple.

residual elastic energy increases. A small amount of energy is released in the form of surface energy, and the rest of the energy is the source of energy for the occurrence of a rock burst. At this time, if the released energy is greater than the energy consumed by the damage, it will easily lead to shock under mining disturbance (such as roof fracture movement, coal blasting, and mechanical vibrations).

2.2.2. Different Foundation Stiffness.

(1) Analysis of anticlinal deflection. When the tectonic couple is $M_0 = 4.0 \times 10^9$ N·m, the foundation stiffness is taken as k = 10 GPa, 15 GPa, and 20 GPa. The corresponding anticlinal deflection curve is shown in Figure 5.

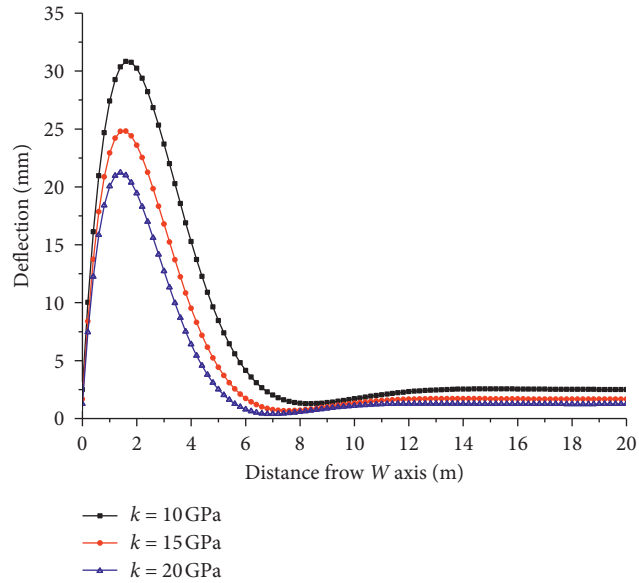

Figure 5: Distribution curves of anticlinal deflection with different foundation stiffness.

It can be seen from Figure 5 that the anticline deflection decreases with increased foundation stiffness when the tectonic couple is constant. The deflection peak is located 2 m from the center of the w-axis. As the distance from the center of the w-axis increases, the deflection value decreases. If key stratum exists in the coal strata, and the stiffness of the key layer is greater, the anticline structure is more difficult to form. However, the greater the stiffness of the key layer stored a large amount of energy, the greater the possibility of rock burst becomes.

(2) Analysis of anticlinal elastic strain energy. When the tectonic couple is $M_0 = 4.0 \times 10^9$ N·m, the foundation stiffness is taken as k = 10 GPa, 15 GPa, and 20 GPa. The corresponding anticlinal elastic strain energy curve is shown in Figure 6.

It can be seem from Figure 6 that the anticlinal elastic strain energy decreases with the increase of foundation stiffness when the tectonic coupling is constant. A large amount of elastic strain energy is stored in the anticlinal wing. When the mining face is pushed into the area, surrounding rock stress increases significantly with the influence of mining, and the stored elastic strain energy is likely to be released suddenly, increasing risk of rock burst.

3. Stress Evolution Law of Anticline Axis with Mining

3.1. Establishment of Numerical Model. Based on the characteristics of anticline structures and rock bursts, the mechanical response of an anticline structure is simulated using UDEC numerical software. Considering the large scope of anticline geological structures, the numerical model is not based on the actual site modeling. The model only studies the response laws for mining coal stress under the influence of anticline tectonic structures. The design

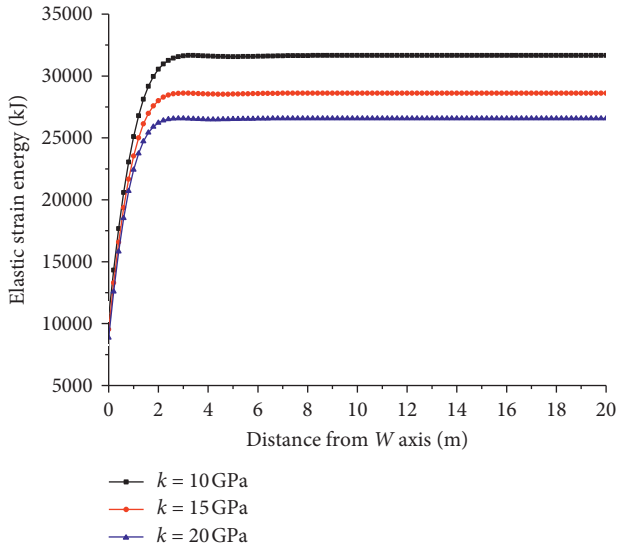

Figure 6: Distribution curves of anticlinal elastic strain energy with different foundation stiffness.

size of the model is 300 m × 180 m in the horizontal and vertical directions. Coal seam thickness is 6 m. Horizontal constraints are applied to the left and right boundaries of the model. The vertical constraint is applied to the bottom boundary. The vertical equivalent load p ($p = \gamma H$) is applied to the top of the model, for simulating the overburdened stratum. Volumetric weight γ is taken 25 kN/m^3. Buried depth of coal seam H is taken 800 m. So, the vertical equivalent load $p = \gamma H = 25\,\text{kN/m}^3 \times 800\,\text{m} = 20\text{MPa}$. The maximum horizontal principal stress is 3–5 times greater than the vertical stress [3]. Therefore, an initial horizontal stress of 60 MPa is applied to simulate the concentrated structure stress in the anticlinal axis. The Mohr–Coulomb model is used to calculate the numerical model. The simplified model is shown in Figure 7.

3.2. Evolution Law of Abutment Pressure. The numerical model is explored step by step in the UDEC numerical software, monitoring the abutment pressure at the range of 60 m in front of the coal wall. With continuous advancement of the working face, the evolution law of abutment pressure in front of the coal wall is obtained as shown in Figure 8, in which negative distance between working face and anticlinal axis indicates that the working face has advanced through the anticlinal axis.

The following can be seen from Figure 8. (1) In Figures 8(a)–(c), with the advancing of working face, the abutment pressure increases significantly by the influence of tectonic stress. (2) When the distance is 4 m between the working face and anticlinal axis in Figure 8(c), the maximum value of the abutment pressure is 60 MPa. (3) When the working face advances through the anticlinal axis in Figure 8(d), the influence range of the abutment pressure decreases.

Through numerical simulation, the "connection-overlay-separation" phenomenon of the abutment pressure is presented between the abutment pressure and the high tectonic stress. It is noted that the abutment pressure in front of the coal wall and high tectonic stress begins to intersect in Figure 8(b). The two overlay each other in Figures 8(b)–8(d), and gradually separate in Figure 8(d).

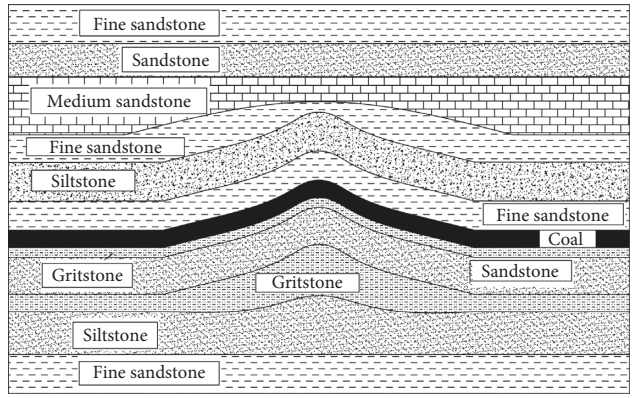

Figure 7: Simplified graphic numerical model.

3.3. Evolution Law of Maximum Principal Stress with Mining Influence. A vertical monitoring line is set up in the anticlinal axis of the numerical model. In the model, 7 monitoring points are established: 3 points are located on the roof (above the coal seam 0.6 m, 7.8 m, and 18.5 m), 3 points are located in the floor strata (below the coal seam 0.53 m, 7.68 m, and 18.42 m), and 1 point is located in the coal seam (above the floor 3.1 m). Using the UDEC numerical software to simulate the process of working face advancement, the evolution curves for the maximum principal stress in the anticlinal axis are shown in Figure 9.

The following can be seen from Figure 9. (1) When the mining face is greater than 40 m from the anticline axis, the coal seam and floor tectonic stress are not affected by the working face advancement. (2) When the mining face is 20–40 m away from the anticline axis, the stress from the coal seam, roof, and floor increases as the working face continues to advance. Additionally, the closer the floor rock is to the coal, the faster the maximum principal stress value increases. (3) Tectonic stress in the anticlinal axis increases rapidly when the distance between the working face and the anticlinal axis is less than 20 m. When the distance between the working face and anticlinal axis is 4 m, the maximum value for the abutment pressure is reached. (4) The roof and floor have some residual stress when the working face advances through the anticlinal axis.

4. Energy Analysis of Rock Burst Risk

4.1. Energy Criterion of Rock Burst. According to the minimum energy principle of rock dynamic failure [33], the failure condition is when the stress exceeds the uniaxial compressive strength, that is $\sigma > \sigma_c$. Meanwhile, the corresponding energy consumption criterion can be expressed as follows:

$$E_c = \frac{\sigma_c^2}{2E}. \tag{8}$$

Research on many rock burst cases has shown that rock bursts often occur in brittle coal and rock. Under the

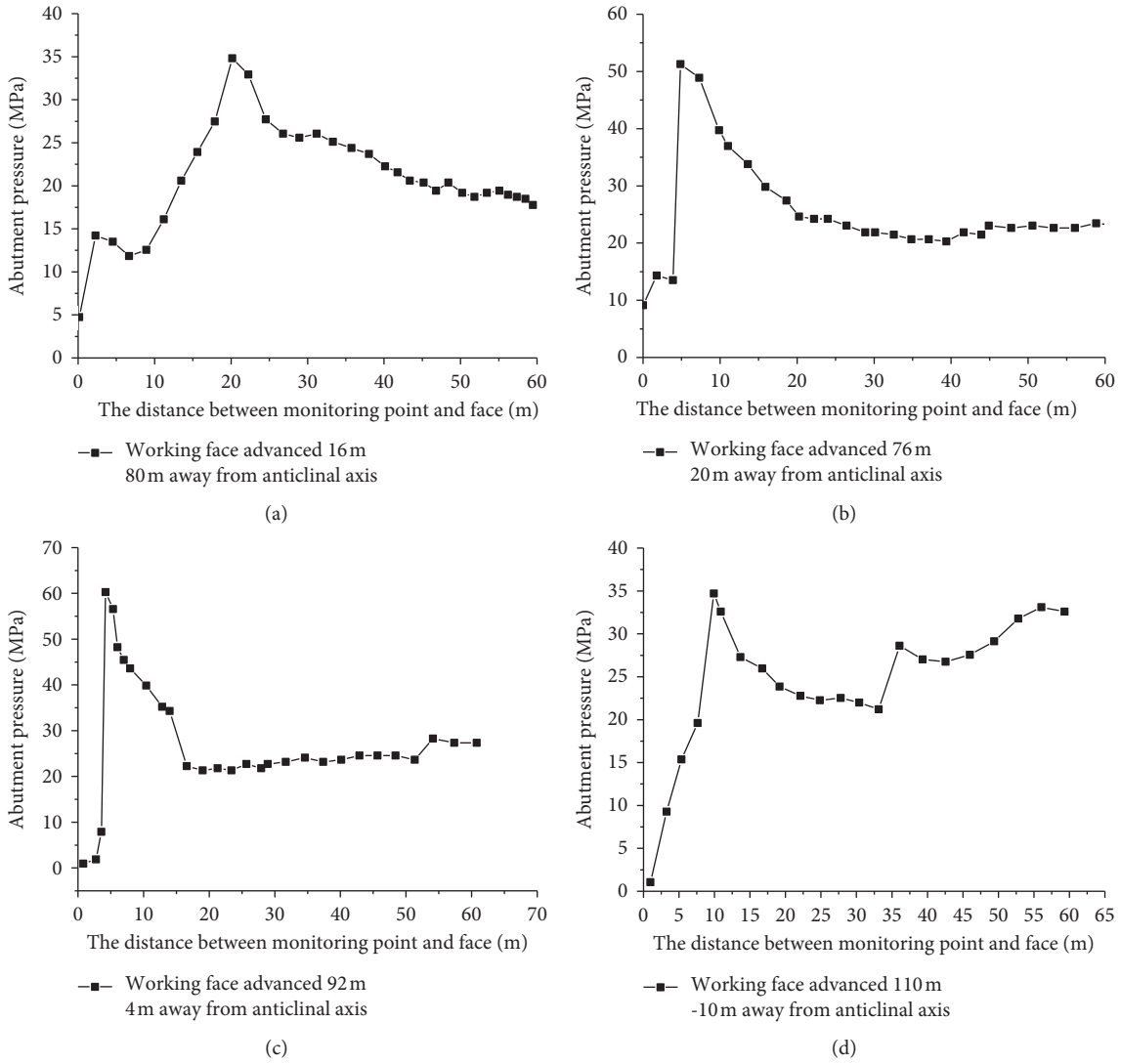

Figure 8: The distribution curves of abutment pressure in front of the coal wall with different advancing distances. (a), (b), (c), and (d).

influence of mining disturbance, this energy can easily be released suddenly, accompanied by the occurrence of shock. Based on the generalized Hook's law, the elastic strain energy of coal in a three-dimensional stress state is calculated as follows:

$$E_0 = \frac{\sigma_1^2 + \sigma_2^2 + \sigma_3^2 - 2\mu\left(\sigma_1\sigma_2 + \sigma_1\sigma_3 + \sigma_3\sigma_2\right)}{2E}, \quad (9)$$

where E is the elastic modulus; μ is Poisson's ratio; and σ_1, σ_2, and σ_3 stand for the first, second, and third principle stresses.

According to the energy theory [34, 35], when the energy released from an unstable coal rock system is greater than the energy consumed, a rock burst will be induced. Therefore, the energy criterion for a rock burst can be established as follows:

$$E_0 - E_c > 0. \quad (10)$$

For specific coal, E and u could be assumed to be constants to a certain extent, in order to theoretically analyze the law of coal seam energy. Therefore, Equations (8), (9), and (10) show that the elastic strain energy depends on the principal stress. When "$E_0 > E_C$," a rock burst may be induced in front of the coal wall.

4.2. Energy Analysis of Rock Burst Danger. The increased area of abutment pressure in front of a coal wall is a serious risk area. Therefore, the numerical calculation mainly studies the impact risk at the peak of abutment pressure. According to the test results for No. 3 coal mechanics, the coal compressive strength is σ_c = 18.8 MPa, the elastic modulus is E = 2.8 GPa, Poisson's ratio is μ = 0.32, and Equation (8) can be solved as E_C = 63.11 kJ/m^3. The stress state of the abutment pressure peak from numerical simulation is shown in Table 1, in which negative distance between working face and anticlinal axis indicates that the working face has advanced through the anticlinal axis, and the corresponding curve "$E_0 - E_C$" is shown in Figure 10.

The following can be seen from Figure 10. (1) When the mining face is greater than 40 m from the anticline axis, the

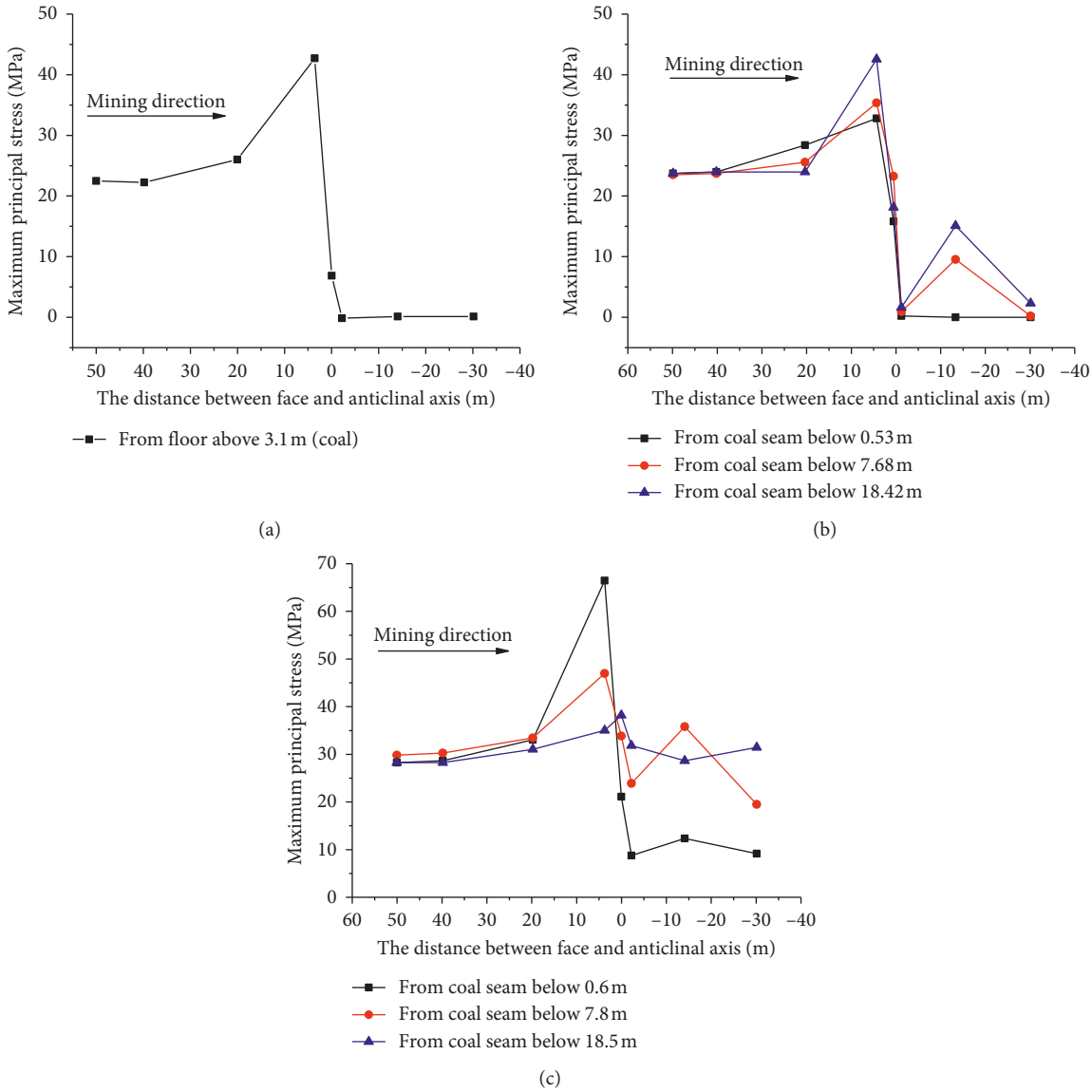

Figure 9: Distribution curves of maximum principal stress of anticlinal axis. (a), (b), and (c).

Table 1: Value of "$E_0 - E_C$" at the peak of abutment pressure with different advancement steps.

Distance between face and anticlinal axis (m)	Maximum principal stress, σ_1 (MPa)	Intermediate principal stress, σ_2 (MPa)	Minimum principal stress, σ_3 (MPa)
60	40.75	15.55	10.51
40	41.93	16.51	14.42
20	51.23	18.89	14.29
4	142.6	14.69	39.08
0	40.76	23.64	14.78
−2	44.00	16.30	11.68
−14	38.19	14.26	9.581
−30	32.62	12.70	8.809

residual energy "$E_0 - E_C$" at the peak of the abutment pressure increases slowly, and the risk of a rock burst is low. (2) In the range of 4–40 m, the residual energy increases rapidly with mining, and the risk of a rock burst begins to increase significantly. (3) When the distance between the working face and anticlinal axis is 4 m, the residual energy "$E_0 - E_C$" reaches a maximum value of 3066.17 kJ/m^3, and the risk of a rock burst is at a maximum. (4) When the working face advances through the anticlinal axis, the value of "$E_0 - E_C$" decreases, so the risk of a rock burst begins to weaken.

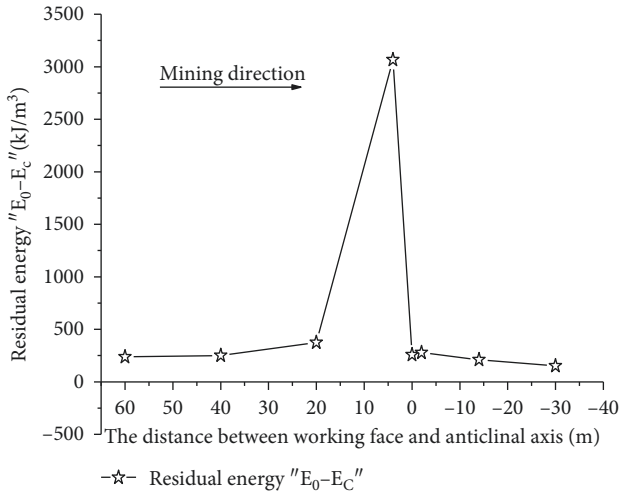

Figure 10: The "$E_0 - E_C$" distribution curve of the abutment pressure peak.

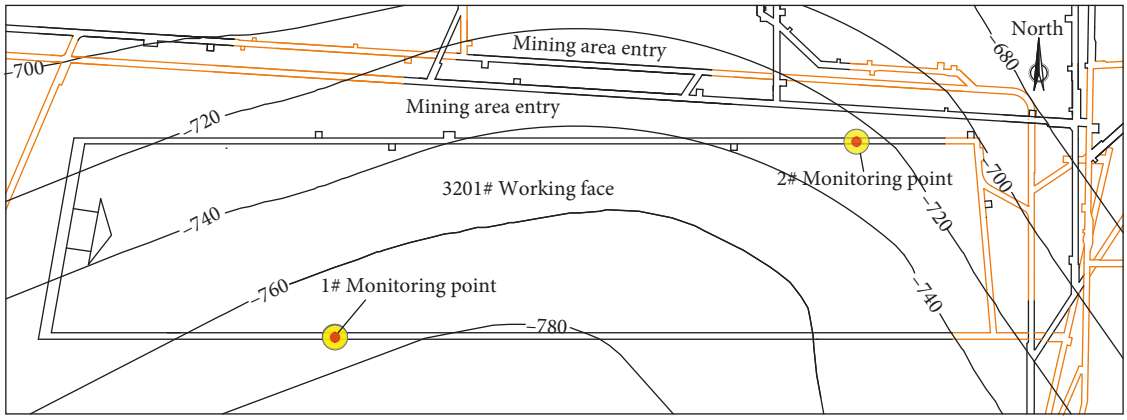

Figure 11: The arrangement diagram of No. 3201 working face microseismic system detector.

5. Field Case

The No. 3201 working face microseismic system detector is arranged as shown in Figure 11. The system monitors microseismic events during the mining period for the working face in an anticlinal structure control area. The microseismic monitoring results are selected during the period from July to September 2016. During this period, the working face advances near the anticlinal axis, pushes to the axis, and eventually pushes through the axis. The events are analyzed statistically as shown in Figure 12.

The following can be seen from Figure 12. (1) When the distance between the working face and the anticlinal axis exceeds 168 m, the coal in front of the working face is less affected by the anticlinial structure. Microseismic events and frequency are mainly affected by the mining factor. (2) When the distance between the face and axis is 104–168 m, the microseismic energy and frequency increase gradually with continuous advancement of the working face to the

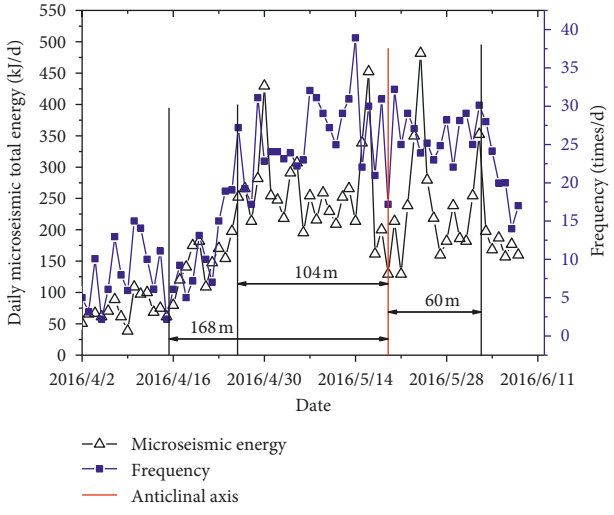

Figure 12: Statistical analysis of No. 3201 working face microseismic events.

axis. (3) When the distance between the face and the axis is less than 104 m, the superposition of high tectonic stress and mining stress causes the abutment pressure to increase significantly, resulting in higher microseismic energy and frequency. (4) When the face advances through the anticlinal axis, reaching 60 m from the axis, the control of the anticline structure is weakened, and the microseismic energy and frequency are also reduced. From this analysis, it can be seen that the variation law for microseismic energy with the distance between the working face and the axis is consistent with the variation law for the residual energy "$E_0 - E_C$" at the peak of the simulated abutment pressure.

6. Conclusions

(1) Based on the Winker elastic foundation theory, a mechanical model for an anticline structure is constructed, and theoretical solutions for the deflection and elastic strain energy of a rock beam are deduced. The distribution features of rock beam deflection and elastic strain energy with the change of foundation stiffness and structural coupling are also evaluated using a control variable method, for exploring internal factors of anticline formation and the associated rock burst.

(2) Affected by high tectonic stress from an anticlinal structure, the "connection-overlay-separation" phenomenon of abutment pressure is presented between the abutment pressure and high tectonic stress with working face advancement. Moreover, the connection area and the overlay area are at serious risk of a rock burst.

(3) While the working face remains close to the anticline axis, the stress from the roof and floor, and the remaining energy value "$E_0 - E_C$" of the abutment pressure peak increases continuously. When the working face advances through the anticlinal axis, the principal stress and residual energy begin to decrease. However, there are still residual stresses, which follow certain law distributions with mining.

(4) The field example shows that the microseismic energy and frequency are affected by high tectonic stress and mining stress, and they increase significantly, which are associated with the possibility of rock bursts.

Data Availability

The data used to support the findings of this study are available from the corresponding author upon request.

Conflicts of Interest

The authors declare that they have no conflicts of interest.

Acknowledgments

This work was supported by the State Key Research Development Program of China (No. 2016YFC0801403), the Shandong Provincial Natural Science Foundation, China (ZR2018MEE009), and Open project fund for State Key Laboratory of Mining Disaster Prevention and Control Cofounded by Shandong Province, and the Ministry of Science and Technology (MDPC2017ZR04). These financial aids are gratefully acknowledged.

References

[1] B. H. G. Brady and E. T. Brown, *Rock Mechanics: For Underground Mining*, Springer, Dordrecht, Holland, Netherlands, 3rd edition, 2004.

[2] S. T. Gu, B. Y. Jiang, Y. Pan, and Z. Li, "Bending moment characteristics of hard roof before first breaking of roof beam considering coal seam hardening," *Shock and Vibration*, vol. 2018, Article ID 7082951, 22 pages, 2018.

[3] Q. X. Qi and L. M. Dou, *Theory and Technology of Rock Burst*, China University of Mining and Technology Press, Xuzhou, China, 2008.

[4] R. Patynska, "The consequences of rock burst hazard for Silesian companies in Poland," *Acta Geodynamica Et Geomaterialia*, vol. 10, no. 2, pp. 227–235, 2013.

[5] T. B. Zhao, W. Y. Guo, Y. L. Tan, C. P. Lu, and C. W. Wang, "Case histories of rock bursts under complicated geological conditions," *Bulletin of Engineering Geology and the Environment*, pp. 1–17, 2017.

[6] G. F. Wang, S. Y. Gong, Z. L. Li, L. M. Dou, W. Cai, and Y. Mao, "Evolution of stress concentration and energy release before rock bursts: two case studies from Xingan Coal mine, Hegang, China," *Rock Mechanics and Rock Engineering*, vol. 49, no. 8, pp. 3393–3401, 2016.

[7] Y. L. Tan, F. H. Yu, J. G. Ning, and T. B. Zhao, "Design and construction of entry retaining wall along a gob side under hard roof stratum," *International Journal of Rock Mechanics and Mining Sciences*, vol. 77, pp. 115–121, 2015.

[8] N. G. W. Cook, E. Hoek, J. P. G. Pretorius, W. D. Ortlepp, and M. D. G. Salamon, "Rock mechanics applied to the study of rock bursts," *Journal of the South African Institute of Mining and Metallurgy*, vol. 65, pp. 437–446, 1965.

[9] A. Z. Hua and M. Q. You, "Rock failure due to energy release during unloading and application to underground rock burst control," *Tunnelling and Underground Space Technology*, vol. 16, no. 3, pp. 241–246, 2001.

[10] B. Jiang, L. Wang, Y. Lu, C. Wang, and D. Ma, "Combined early warning method for rockburst in a Deep Island, fully mechanized caving face," *Arabian Journal of Geosciences*, vol. 9, no. 20, p. 743, 2016.

[11] A. V. Dyskin and L. N. Germanovich, "Model of rockburst caused by cracks growing near free surface," in *Rockbursts and Seismicity in Mines*, R. P. Young, Ed., pp. 169–174, Rotterdam, Balkema, 1993.

[12] X. C. Zhang, A. H. Lu, and J. Q. Wang, "Numerical simulation of layer-crack structure of surrounding rock and rock burst in roadway under dynamic disturbance," *Chinese Journal of Rock Mechanics and Engineering*, vol. 25, no. S1, pp. 3110–3114, 2006.

[13] Q. X. Huang and S. N. Gao, "The damage and fracture mechanics model of roadway rock burst," *Journal of China Coal Society*, vol. 26, no. 2, pp. 156–159, 2001.

[14] Y. Pan, Y. Liu, and S. F. Gu, "Fold catastrophe model of mining fault rock burst," *Chinese Journal of Rock Mechanics and Engineering*, vol. 20, no. 1, pp. 43–48, 2001.

[15] X. S. Liu, Y. L. Tan, J. G. Ning, Y. W. Lu, and Q. H. Gu, "Mechanical properties and damage constitutive model of

coal in coal-rock combined body," *International Journal of Rock Mechanics and Mining Sciences*, vol. 110, pp. 140–150, 2018.

[16] A. M. Linkov, "Equilibrium and stability of rock masses," *Eighth International Congress on Rock Mechanics*, vol. 3, pp. 1049–1054, 1997.

[17] W. Y. Guo, Y. L. Tan, F. H. Yu et al., "Mechanical behavior of rock-coal-rock specimens with different coal thicknesses," *Geomechanics and Engineering*, vol. 15, no. 4, pp. 1017–1027, 2018.

[18] Z. C. Zhu, B. Z. Wei, and S. Zhang, *Structural Geology*, China University of Geosciences Press, Beijing, China, 1999.

[19] Aweil, *Rock Burst, China Coal Industry*, Publishing Home, Beijing, China, 1959.

[20] S. M. Lee, B. S. Park, and S. W. Lee, "Analysis of rock bursts that have occurred in a waterway tunnel in Korea," *International Journal of Rock Mechanics and Mining Sciences*, vol. 3, no. 41, pp. 1–6, 2004.

[21] T. B. Zhao, W. Y. Guo, Y. L. Tan, Y. C. Yin, L. S. Cai, and J. F. Pan, "Case studies of rock bursts under complicated geological conditions during multi-seam mining at a depth of 800 m," *Rock Mechanics and Rock Engineering*, vol. 51, no. 5, pp. 1539–1564, 2018.

[22] L. Chen, P. Li, G. Liu, W. Cheng, and Z. Liu, "Development of cement dust suppression technology during shotcrete in mine of China-A review," *Journal of Loss Prevention in the Process Industries*, vol. 55, pp. 232–242, 2018.

[23] Y. L. Tan, F. H. Yu, and L. Chen, "A new approach for predicting bedding separation of roof strata in underground coalmines," *International Journal of Rock Mechanics and Mining Sciences*, vol. 61, pp. 183–188, 2013.

[24] S. T. Gu, Z. M. Xiao, and R. F. Huang, "Danger mechanism of rock burst induced by mining in synclinal influence area," *Electronic Journal of Geotechnical Engineering*, vol. 20, no. 12, pp. 5103–5114, 2015.

[25] V. Frid, "Calculation of electromagnetic radiation criterion for rock burst hazard forecast in coal mines," *Pure and Applied Geophysics*, vol. 158, no. 5, pp. 931–944, 2001.

[26] G. C. Zhang, S. J. Liang, Y. L. Tan, F. X. Xie, S. J. Chen, and H. G. Jia, "Numerical modeling for longwall pillar design: a case study from a typical longwall panel in China," *Journal of Geophysics and Engineering*, vol. 15, no. 1, pp. 121–134, 2018.

[27] S. K. Sharan, "A finite element perturbation method for the prediction of rock burst," *Computers and Structures*, vol. 85, no. 17, pp. 1304–1309, 2007.

[28] P. K. Kaiser and M. Cai, "Design of rock support system under rock burst condition," *Journal of Rock Mechanics and Geotechnical Engineering*, vol. 4, no. 3, pp. 215–227, 2012.

[29] A. C. Adoko, G. Gokceoglu, L. Wu, and Q. J. Zuo, "Knowledge-based and data-driven fuzzy modeling for rock burst prediction," *International Journal of Rock Mechanics and Mining Sciences*, vol. 61, no. 7, pp. 86–95, 2013.

[30] G. S. Zhang, "Structural characteristics of Yanshan period of Southeastern Hubei and it's rock control and ore control," *Hubei Geology*, vol. 6, no. 2, pp. 16–29, 1992.

[31] C. Zhang, "Study on the stages and force sources of tectonic stress field in Wuxu ore area, Hechi City, Guangxi," *Guangxi Geology*, vol. 13, no. 2, pp. 7–10, 2000.

[32] Q. L. Wang, M. C. Yun, and H. S. Wang, "Characteristics and its formation analysis of Taiyuan tilting structure," *North Western Geology*, vol. 43, no. 3, pp. 41–46, 2010.

[33] Y. S. Zhao, Z. C. Feng, and Z. J. Wan, "Least energy principle of dynamical failure of rock mass," *Chinese Journal of Rock Mechanics and Engineering*, vol. 22, no. 11, pp. 1781–1783, 2003.

[34] H. P. Xie, Y. Ju, and L. Y. Li, "Criteria for strength and structural failure of rocks based on energy dissipation and energy release principles," *Chinese Journal of Rock Mechanics and Engineering*, vol. 24, pp. 3003–3010, 2005.

[35] N. G. W. Cook, "A note on rockburst considered as a problem of stability," *Journal of South African Institute of Mining and Metallurgy*, vol. 65, pp. 437–446, 1965.